

Gamma activity in human EEG is related to high-speed memory comparisons during object selective attention

Christoph S. Herrmann and Axel Mecklinger

Max-Planck Institute of Cognitive Neuroscience, Leipzig, Germany

Among the most important processes of the brain in order to correctly perceive the outside world and act within it are binding, attention, and memory. All three functional mechanisms have been associated with brain activity in the gamma frequency range. It needs to be clarified, however, which subprocesses within the gamma frequency range relate to which perceptual or cognitive functions. In a visual discrimination task, we used Kanizsa figures whose constituent inducer disks need to be bound together to perceive the illusory contours. By a variation of the task requirements we manipulated the allocation of object selective attention as compared to a previous study. One out of four objects had to be detected. This detection process requires the comparison of two object dimensions (form and collinearity) with a working memory template. In order to get behavioural and electrophysiological measures, EEG and reaction times were recorded from 16 and 10 subjects, respectively. We demonstrated that the early evoked gamma activity reflects the process of allocating attention to a selected object as early as 50–150 ms after stimulus onset. We propose that the underlying mechanism is a high-speed memory comparison. In addition, we show that this early gamma activity also determines the reaction times needed to respond to the different stimuli.

INTRODUCTION

Binding and attention are both necessary for the correct function of perceptual processes in the brain. Binding is necessary to link together the different features of single objects that are represented in a distributed fashion in the brain.

Please address all correspondence to C. Herrmann, Max-Planck Institute of Cognitive Neuroscience, PO Box 500 355, 04303 Leipzig, Germany. Email: herrmann@cns.mpg.de

We would like to thank Mark A. Elliott for his editorial work and three anonymous referees for valuable comments on an earlier version of this manuscript. We also express our thanks to Diana Böttger who helped to prepare the experimental set up, to Cornelia Schmidt for collecting the data, and to Andrea Sandmann who helped to design the figures. Diana Böttger was partly supported by DFG grant SCHR 375/8-1.

The mechanism of attention serves to focus onto a small subset of the vast amount of incoming information. It is still unclear how exactly these two mechanisms operate or interact. Binding is believed to operate at a very early stage in human information processing. According to the temporal correlation hypothesis, the simultaneous firing of neurons indicates that they code features of the same object (Singer & Gray, 1995; von der Malsburg & Schneider, 1986). Electrophysiological studies on humans and animals show strong evidence that brain activity in the gamma frequency range (approximately 30–80 Hz, mostly 40 Hz) could be the correlate of feature binding (Gray, König, Engel, & Singer, 1989; Tallon-Baudry & Bertrand, 1999). Nevertheless, it has been questioned whether gamma activity in the human electroencephalogram (EEG) really reveals processes of feature binding or rather relates to memory access (Pulvermüller, Keil, & Elbert, 1999).

If binding elicits gamma activity in the brain it seems plausible to assume that stimuli which oscillate at a frequency in the gamma range result in enhanced processing by the brain. This led to an experiment of Elliott and Müller (1998) who demonstrated that stimuli flickering in the gamma range can enhance visual binding. In that study, Kanizsa-like figures had to be detected and reaction time (RT) significantly decreased when target-relevant cues were preattentively flickering at a frequency of 40 Hz prior to the detection period, as compared to other flickering frequencies. Further investigation by Elliott and Müller (2000) with the same paradigm has revealed that an object representation persisted with a 40 Hz oscillatory code for several hundred milliseconds. These findings are in line with previous results about high-speed memory processes in the same frequency range: Jensen and Lisman (1998) demonstrated in simulations that high-speed access to working memory may operate at frequencies in the gamma range, and Burle and Bonnet (2000) performed an auditory interference task suggesting an oscillatory process in working memory. The paradigm of Elliott and Müller also evokes gamma oscillations in the human EEG that determine the enhanced processing when target-relevant cues are presented (Elliott, Herrmann, Mecklinger, & Müller, 2000).

Gamma activity has not only been correlated with binding and memory, but there is also evidence that the same type of activity correlates with attention (Başar-Eroglu, Strüber, Schürmann, Stadler, & Başar, 1996; Müller, Gruber, & Keil, 2000; Tiitinen et al., 1993). In a recent EEG-experiment, Herrmann, Mecklinger, and Pfeiffer (1999) showed that an early gamma response in a visual discrimination task was larger for target stimuli than for non-target stimuli. In that experiment, Kanizsa squares and triangles (Kanizsa, 1976) as well as non-Kanizsa squares and triangles were visually presented to the subjects. The four different stimuli (Figure 1) were comprised of the two features form (3 vs. 4 inducer disks) and collinearity (presence/absence of an illusory Kanizsa figure due to collinear arrangement of the inducer disks). The authors formulated

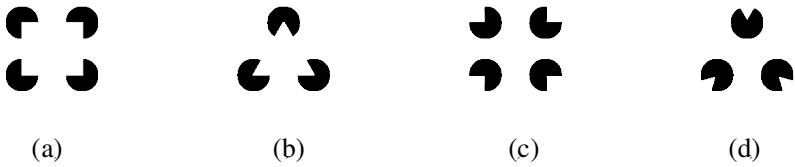


Figure 1. The four stimulus types used in the experiment: (a) Kanizsa square, (b) Kanizsa triangle, (c) non-Kanizsa square (target), and (d) non-Kanizsa triangle.

the hypothesis that the target effect of the early gamma activity was reflecting an attentional top-down process of stimulus selection.

The objective of the present experiments was to further investigate the possibility of early gamma activity reflecting a process of object-selective attention. Especially, we wanted to investigate how such a process operates and interacts with working memory. In our experiments, we used the identical four stimuli used in the study of Herrmann et al. (1999) but changed the task requirements for the subjects. Whereas Herrmann et al. (1999) used the Kanizsa square as the target, we here defined the non-Kanizsa square as the target that had to be counted. If the assumption is true, that the early gamma activity reflects an attentional process of object selection, it should be largest for the non-Kanizsa square in our new experiment. The amplitude of the visual N170 (negative deflection around 170 ms) was assumed to reflect physical and perceptual properties of the stimuli in the experiment of Herrmann et al. (1999). If this is true, the order of N170 amplitude for the four stimuli should not change in our new experiment. The event-related potential P300 (positive deflection around 300 ms) is known to reflect attentional mechanisms and to be maximal in response to infrequent targets (Donchin & Coles, 1988; Mecklinger & Ullsperger, 1993). Thus, the P300 should also be largest for the non-Kanizsa square. In order to gain additional insights in the attentional mechanism engaged in object selection, we also recorded RTs from another group of subjects performing the same task.

In a previous experiment with the four previously-mentioned stimuli, in which MEG and RTs were recorded simultaneously, Herrmann and Mecklinger (2000) demonstrated that targets (Kanizsa squares) were processed slowest even though they constituted a Kanizsa figure, whereas faster non-targets did not constitute Kanizsa figures. The RT pattern suggested a two-fold mechanism of comparing the two dimensions form and collinearity of an encoded stimulus with a pattern held in working memory. The stimulus which was most dissimilar to the target (non-Kanizsa triangle) was processed fastest in their experiment. In our new experiment, we defined the non-Kanizsa square as the target and expected it to be processed slowest, whereas we expected the most dissimilar stimulus (Kanizsa triangle) to be processed fastest.

METHODS

In our EEG experiment, subjects had to count the occurrence of target stimuli among non-target stimuli. This made the experiment comparable to the one of Herrmann et al. (1999) and keeps EEG responses free from motor artefacts. In order to also acquire behavioural measures of the task, we conducted an additional reaction-time experiment (RT experiment). In the RT experiment subjects had to respond with their right index finger to targets and with their left index finger to non-targets, yielding RTs and error measures under stimulation conditions identical with the EEG experiment.

Subjects

Sixteen subjects with a mean age of 22.6 years (ranging from 18 to 26 years, 7 female) participated in the EEG experiment and ten subjects with a mean age of 23.1 years (ranging from 19 to 31 years, 7 female) participated in the RT experiment. All subjects were right-handed and had normal or corrected-to-normal vision. They showed no signs of neurological or psychiatric disorders and all gave written informed consent to participate in the study.

Stimuli

The stimuli used in this paradigm were composed of three or four inducer disks, which either constitute a Kanizsa figure due to their collinear arrangement (Figure 1a and b) or don't constitute one (Figure 1c and d). The stimuli were identical to those of Herrmann et al. (1999) and varied across two dimensions, which we will refer to as form and collinearity dimension. The dimension "form" determines whether a stimulus is composed of three or four inducer disks, whereas the dimension "collinearity" determines whether a stimulus constitutes a Kanizsa figure due to the collinear arrangement of its inducer disks.

The stimuli were presented for 700 ms with randomized intertrial-intervals ranging from 1000 to 1500 ms. Figures were displayed in black together with a black central fixation cross on white background. Stimuli subtended a visual angle of $4^{\circ}17'$ including inducer disks, while the induced illusory figures subtended $2^{\circ}86'$ (Figure 2). Thus, the whole stimulus is projected into the field of central vision, i.e., the central 5 degrees of the macular region (Zeki, 1993). Fixation crosses were displayed foveally (0.02°). The ratio of the radius of the inducer disks and the side-length of the illusory figures was 1:4.

Figures were displayed on a computer monitor placed 1 m in front of the subjects. Subjects were instructed to silently count the appearance of the non-Kanizsa square (targets). The experiment was run in four blocks with 100 stimuli per block. The four stimulus types were presented equally probable in a pseudo-randomized order resulting in a target probability of .25.

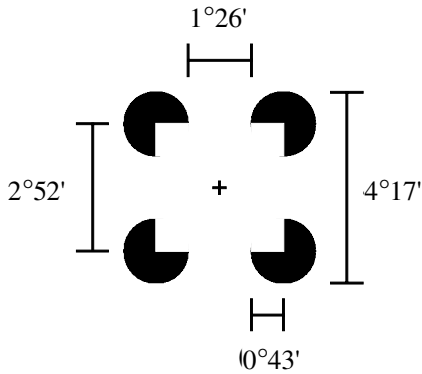


Figure 2. Size of the used stimuli in visual degrees.

Data acquisition

The EEG was recorded with NeuroScan amplifiers using 64 tin electrodes mounted in an elastic cap. Electrodes were placed according to the international 10-10 system. The ground electrode was placed near the left mastoid (M1) and all electrodes were referenced to the left mastoid. Electrode impedance was kept below $5\text{k}\Omega$. Horizontal and vertical electrooculogram (EOG) recordings were registered with four additional electrodes. Data were sampled at 500 Hz and analog-filtered with a 0.05 Hz high-pass and a 100 Hz low-pass filter. An additional, digital 20 Hz low-pass filter was applied before displaying the ERP data.

Averaging epochs lasted from 200 ms before to 900 ms after stimulus onset. All epochs were visually inspected for artefacts and rejected if eye-movement artefacts, muscle artefacts, or electrode drifts were visible. Three subjects had to be excluded from further analysis due to excessive eye-movements. Baselines were computed in the $-200-0$ ms interval in each single trial and subtracted prior to computing the event-related potential (ERP) averages.

Data analysis

For the interpretation of gamma activity it is assumed to be important that the oscillations occur either phase-locked to a stimulus (evoked activity) or with variable phase relative to a stimulus (induced activity). For the analysis of gamma activity, a wavelet transform based on Morlet wavelets was employed (Herrmann et al., 1999). To differentiate between evoked and induced activity, each subject's ERP is transformed yielding evoked gamma activity and averages of transforms of single epochs are computed yielding induced activity.

In order to avoid a loss of statistical power that is inherent when repeated measures ANOVAs are used to quantify multi-channel EEG data (Oken & Chiappa, 1986), selected electrode sites were pooled to four topographical regions of interest (ROIs). The left anterior region (LAR) was comprised of electrodes FP1, F7, F3, F5, AF7, and FC3; the left posterior region (LPR) included electrodes P7, P5, P3, PO7, PO3, and O1. Regions over the right hemisphere included the homologous electrodes. For statistical analyses, ERP amplitudes were pooled across the electrodes in each of the ROIs. ERP components were defined as mean amplitudes in the following time intervals: 130–180 ms (N170) and 300–500 ms (P300).

EEG data was analysed with two ANOVAs: In one of them, the two stimulus dimensions form and collinearity were used as factors with levels square vs. triangle and collinear vs. non-collinear, respectively. We will refer to this type of ANOVA as stimulus-ANOVA, since it differentiates between the features of a stimulus. In addition, we computed a second type of ANOVA contrasting the target with the mean of the three non-targets. We will refer to this as the response-ANOVA, since it reflects the response requirements. (See Table 1.) ANOVAs conducted for EEG data had an additional factor topography (anterior, posterior).

These repeated-measures ANOVAs were also computed for RTs and error rates of the RT experiment. RTs on trials in which a response error was made, were rejected from the data, as well as trials in which the RT exceeded 2.5 standard deviations of the mean.

Before analysing gamma responses, we evaluated the signal-to-noise ratio (SNR) of the time interval to be analyzed. In order to achieve this, we computed SNR-ANOVAs to determine whether the mean amplitude in specific time intervals (50–150 ms and 200–300 ms) differs significantly from the noise in the baseline (–100–0 ms). Only if this is the case, subsequent ANOVAs which test variations due to experimental conditions make sense.

TABLE 1
Overview of the statistical tests for the experimental variables

<i>Statistical test</i>	<i>Factors</i>	<i>Factor level</i>
Stimulus-ANOVA	form collinearity	(Kan4, Non4) vs. (Kan3, Non3) (Kan4, Kan3) vs. (Non4, Non3)
Response-ANOVA	targetness	Non4 vs. (Kan4, Kan3, Non3)

The four figural stimuli are abbreviated as Kan (Kanizsa figures) and Non (non-Kanizsa figures) and numbers indicate the number of inducer disks.

RESULTS

Behavioural data

The response-ANOVA for the RTs of the RT experiment yielded a significant main effect, $F(1, 9) = 16.58, p < .005$, demonstrating that targets are processed slower (665 ms) than non-targets (632 ms). The stimulus-ANOVA yielded significant effects of collinearity, $F(1, 9) = 16.27, p < .005$, and form, $F(1, 9) = 42.26, p < .0001$, indicating longer RTs for squares than for triangles as well as longer RTs for non-Kanizsa figures than Kanizsa figures. In addition, the stimulus-ANOVA yielded a significant collinearity \times form interaction, $F(1, 9) = 9.96, p = .01$. Post-hoc comparisons revealed that within the triangles there is a significant effect of collinearity, $F(1, 9) = 65.73, p < .0001$, but not within the squares (Figure 3, left).

The response-ANOVA for the error rates yielded a significant main effect of targetness, $F(1, 9) = 15.98, p < .005$, indicating more errors for targets (7.4%) than for non-targets (3.4%). The stimulus-ANOVA of the error rates yielded a significant form effect, $F(1, 9) = 14.70, p < .005$, revealing that error rates are higher for squares than for triangles. Basically, the pattern of the error rates resembles that of the RTs (Figure 3, right). The fact that the pattern of errors is not inverse to that of RTs indicates that we are not dealing with a speed-accuracy trade-off, but an effect of feature processing (Pachella, 1974).

ERP responses

Figure 4 shows the ERPs at selected electrodes over frontal, central, parietal, and occipital areas. In all conditions, there is a prominent N170 peak around 170 ms which is strongest in occipital electrodes. An additional P300 peaks around 400 ms and is strongest for the target condition.

The stimulus-ANOVA for the time interval of the N170 yielded significant effects of collinearity, $F(1, 12) = 39.12, p < .0001$, and form, $F(1, 12) = 13.40, p < .005$. Amplitudes were larger for squares than for triangles and larger for

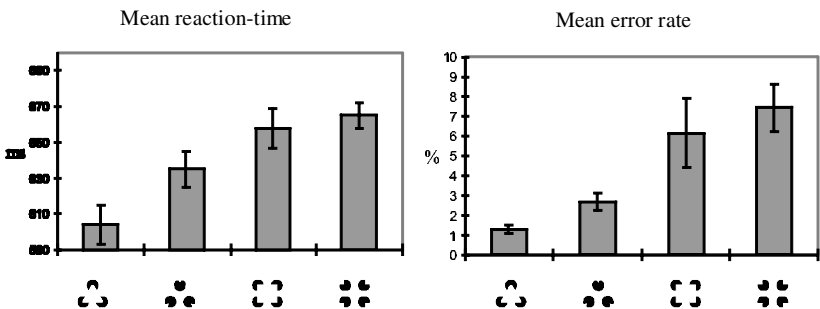


Figure 3. Mean RTs and error rates (means and standard errors of means) for the RT experiment.

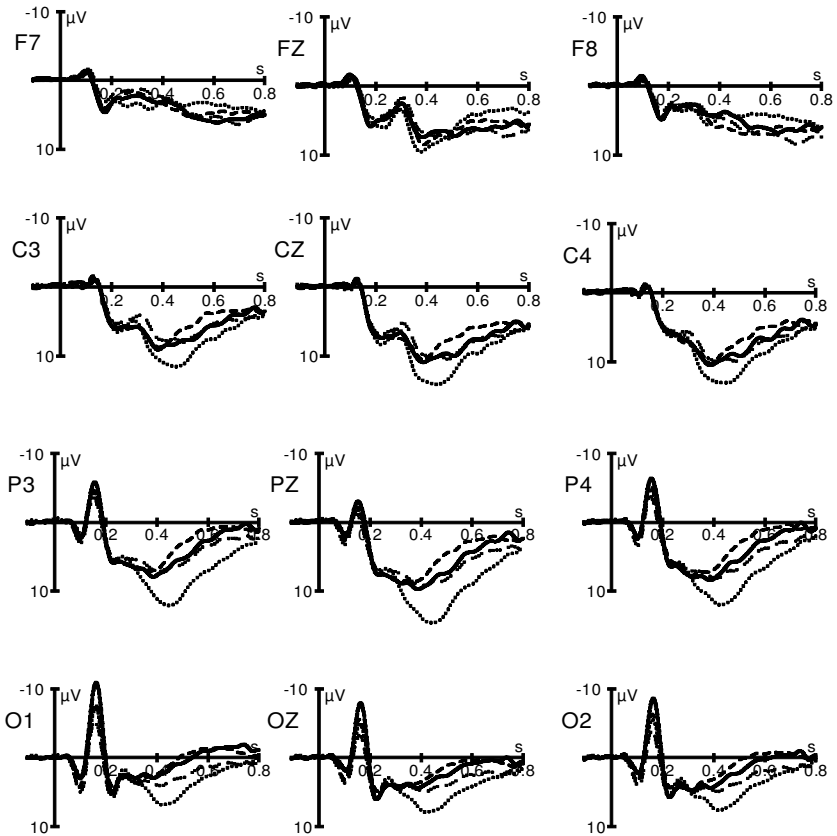


Figure 4. 20 Hz low-pass filtered ERPs averaged across 13 subjects in response to Kanizsa squares (solid), Kanizsa triangles (dashed), non-Kanizsa squares (target, dotted), and non-Kanizsa triangles (intermittently dotted).

Kanizsa figures than non-Kanizsa figures. A significant interaction of Topography \times Collinearity, $F(1, 12) = 7.65$, $p < .05$, revealed that the collinearity effect was much stronger at posterior electrodes, $F(1, 12) = 28.02$, $p < .0005$, than in anterior ones, $F(1, 12) = 9.40$, $p < .01$. The post-hoc tests revealed that, even though the Topography \times Form interaction was not significant in the ANOVA, a form main effect was significant at posterior electrodes, $F(1, 12) = 9.77$, $p < .01$. The order of response magnitude of the N170 was the same as in the previous experiment by Herrmann et al. (1999) as can be seen from the direct comparison in Figure 5. The order was: > Kanizsa square (7.9 μV) > Kanizsa triangle (6.4 μV) > non-Kanizsa square (5.9 μV) > non-Kanizsa triangle (4.5 μV); amplitudes were averaged across posterior electrodes. The response-ANOVA yielded no significant effect.

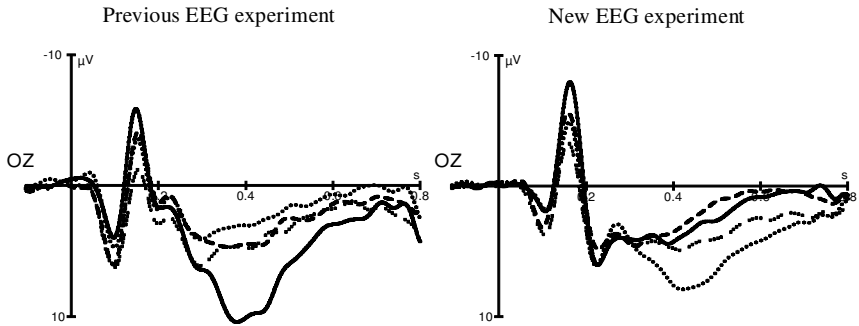


Figure 5. ERPs of electrode OZ for experiments 1 and 2. N170 components are independent of task requirements. The P300 component is affected by the task change between experiments and is delayed in latency and reduced in amplitude.

The response-ANOVA for the time interval of the P300 yielded a significant main effect for targetness, $F(1, 12) = 14.39, p < .005$, indicating larger potentials for targets ($6.6 \mu\text{V}$, amplitudes averaged across all electrodes) than non-targets ($5.0 \mu\text{V}$). A significant interaction of Topography \times Targetness, $F(1, 12) = 7.80, p < .05$, justified post-hoc comparisons in the different regions. The target effect was only significant at posterior electrodes, $F(1, 12) = 27.30, p < .0005$, but not in anterior ones, $F(1, 12) = 0.12$. The stimulus-ANOVA yielded significant main effects of form, $F(1, 12) = 16.96, p < .005$, squares ($6.3 \mu\text{V}$) being greater than triangles ($5.2 \mu\text{V}$), and collinearity, $F(1, 12) = 4.75, p < .05$, collinear ($5.4 \mu\text{V}$) figures being greater than non-collinear ones ($6.2 \mu\text{V}$). Significant interactions were found for Topography \times Form, $F(1, 12) = 6.91, p < .05$, Topography \times Collinearity, $F(1, 12) = 5.36, p < .05$, and Form \times Collinearity, $F(1, 12) = 5.61, p < .05$. Post-hoc comparisons in the individual regions revealed significant effects of form, $F(1, 12) = 20.42, p < .001$, squares ($6.5 \mu\text{V}$) being greater than triangles ($4.7 \mu\text{V}$) and collinearity, $F(1, 12) = 12.40, p < .005$, collinear ($4.9 \mu\text{V}$) figures being greater than non-collinear ones ($6.3 \mu\text{V}$) in posterior electrodes but no effects in anterior electrodes.

In the previous EEG experiment by Herrmann et al. (1999), the target-P300 had a latency of 382 ms and an amplitude of $18.1 \mu\text{V}$ at the PZ recording site. In the present EEG experiment, P300 latency was delayed (444 ms) and its amplitude reduced ($14.5 \mu\text{V}$).

Gamma responses

The SNR-ANOVA for the evoked gamma activity yielded a significant effect of SNR for the early time interval (50–150 ms), $F(1, 12) = 11.52, p < .01$, but not for the late time interval (200–300 ms). This is illustrated for three electrodes (O1, OZ, and O2) in Figure 6. A clear peak can be seen for three of the four

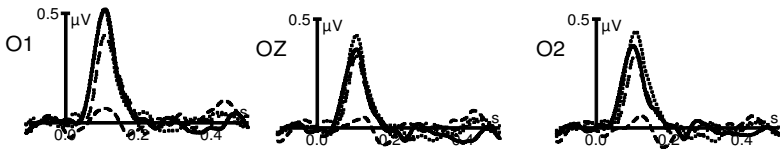


Figure 6. Grand average of the evoked gamma activity across 13 subjects in electrodes, O1, OZ, and O2. A clear peak is visible around 100 ms after stimulus onset.

conditions with a maximum around 100 ms. No difference from baseline is visible after this peak.

The SNR-ANOVA for the induced gamma activity yielded no significant effects. This implies that the SNR of induced gamma activity did not differ from the pre-stimulus baseline period. For this reason we refrained from further analysis of induced gamma activity. The induced gamma activity is illustrated for three electrodes (O1, OZ, and O2) in Figure 7 where no clear peaks can be seen that differ from the baseline activity.

The response-ANOVA for the time interval 50–150 ms of the evoked gamma activity yielded a significant main effect of targetness, $F(1, 12) = 4.93$, $p < .05$, indicating larger gamma activity for the target as compared to the non-targets. The stimulus-ANOVA yielded a significant main effect for form, $F(1, 12) = 5.04$, $p < .05$, indicating larger amplitudes for squares than for triangles. The topographical distribution of the early evoked gamma response is displayed in Figure 8.

Figure 9 shows the total amount of early evoked gamma activity summed across all analysed electrodes for the four conditions. It is obvious that the pattern resembles that of RTs and error rates, i.e., early evoked gamma activity is stronger the more similar a stimulus is to the target. A correlation analysis of the early evoked gamma activity (50–150 ms, averaged across all electrodes and 13 subjects) and the RTs (averaged across 10 subjects) of the four conditions ($n = 4$) revealed a correlation coefficient of 0.9749 ($p < .05$). Notably, the correlation of 0.18 between RT and N170 amplitude was not significant.

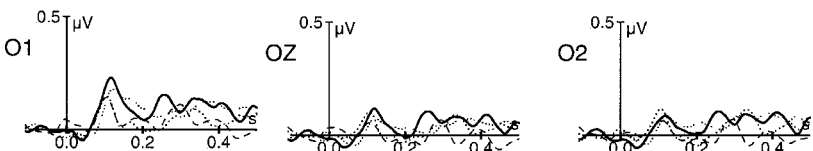


Figure 7. Grand average of the induced gamma activity across 13 subjects in electrodes, O1, OZ, and O2. No clear difference from baseline activity can be observed.

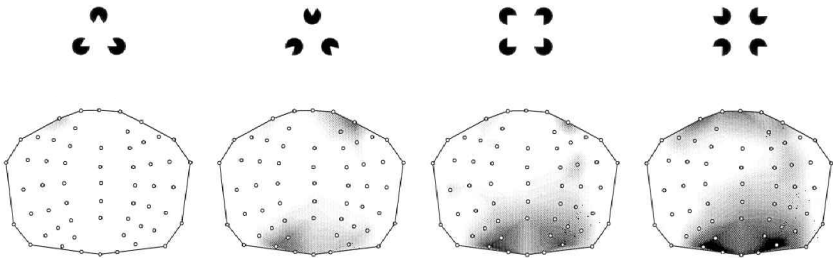


Figure 8. Topography of the early evoked gamma activity for the conditions Kanizsa triangle, non-Kanizsa triangle, Kanizsa square, and non-Kanizsa square (from left to right) in the time interval 50–150 ms averaged over 13 subjects. Gray-scale is from 0 μV (white) to 0.5 μV (black).

DISCUSSION

Behavioural data

From the behavioural data we can see that RTs and error rates show a typical pattern of target discrimination. As expected, the target, which occurs less frequently than the non-targets, is processed slowest (Teichner & Krebs, 1974). In a previous experiment by Herrmann and Mecklinger (2000) this was even the case when the Kanizsa square was the target which would otherwise be expected to be processed faster than a non-Kanizsa square due to its figural features (Pomerantz, 1983). As has been argued by Herrmann and Mecklinger (2000), the pattern of RTs is considered to represent a classification of the targets according to the two dimensions form and collinearity. In our new experiment, the Kanizsa-triangle is dissimilar in both dimensions which define the target: It is composed of three instead of four inducer disks (form) and in contrast to the target constitutes a Kanizsa figure (collinearity). Therefore, it is

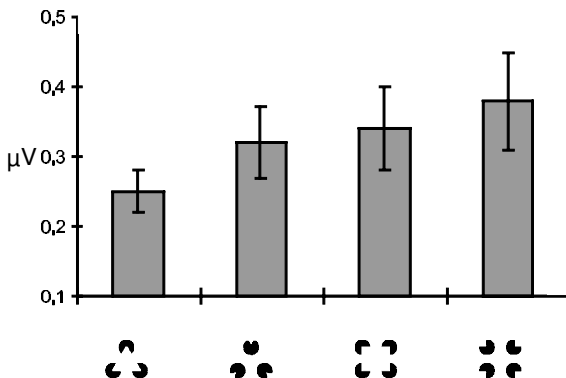


Figure 9. Total amount of early evoked gamma activity (50–150 ms) summed across all analysed electrodes as a function of experimental condition.

the easiest figure to differentiate from the target and by this is processed fastest. The fact that the non-Kanizsa triangle is processed faster than the Kanizsa square, even though they are both dissimilar from the target in one dimension, suggests that the selection process for target discrimination operates as a two-fold mechanism. This mechanism seems to include separate selection processes for comparisons of form and collinearity of the encoded stimulus with a template held in working memory. The fact that error rates did not differ significantly when stimuli varied only across the dimension collinearity while they did differ significantly when stimuli varied across the dimension form might be taken to indicate that the dimension form is more salient to the human visual system. This would also explain why the Kanizsa squares are processed slower than the non-Kanizsa triangles that both share one dimension with the target: The Kanizsa square varies across the less salient dimension collinearity, whereas the non-Kanizsa triangle varies across the more salient dimension form.

ERP responses

The order of N170 amplitude is the same as in the previous experiment by Herrmann et al. (1999) as can be seen from the direct comparison in Figure 5 (Kanizsa square > Kanizsa triangle > non-Kanizsa square > non-Kanizsa triangle). From the previous experiment it could have been concluded that the N170 reflects perceptual processes of illusory contour detection, since the N170 was larger for Kanizsa figures as compared to non-Kanizsa figures. But this effect might have been confounded by the Kanizsa square being the target, since attentional selection processes are known to sometimes influence early ERP components (Heinze et al., 1994). In our new experiment, the order of N170 amplitude did not change relative to the former experiment: The target now evoked the second smallest N170 amplitude showing that in our paradigm the N170 does not reflect attentional selection mechanisms. Thus, since the change in task requirements did not affect the order of N170 amplitude, the collinearity effect is really due to the collinearity of the stimuli and not a confound of the target. This nicely demonstrates that the N170 is driven by physical stimulus properties rather than task requirements. It is noteworthy that the N170 reflects not only physical stimulus properties (three vs. four inducer disks) but also perceptual features like the presence of illusory contours. This effect also suggests that illusory contours are in fact processed by the subjects.

The order of N170 amplitude which stays constant across experiments despite changes in task requirements also indicates that the stimuli possess a certain salience to our visual system. According to the order of N170 amplitude, stimuli that are composed of more inducer disks and stimuli which constitute illusory contours appear to be more salient.

The P300 showed a clear target effect in our EEG experiment. But it was delayed in latency and reduced in amplitude as compared to the previous EEG experiment (Herrmann et al., 1999). This suggests that the detection of the non-Kanizsa square is harder than the detection of the Kanizsa square which is more salient according to our above definition.

Gamma responses

It has been previously stated that the early evoked gamma activity is a purely stimulus-driven component, not being sensitive to perceptual/cognitive functions (Karakas & Başar, 1998). In addition, comparable experiments with Kanizsa and non-Kanizsa figures failed to demonstrate differences between experimental conditions (real triangle, illusory triangle, non-triangle) in the early evoked gamma activity and the effects of targetness were not investigated (Tallon, Bertrand, Bouchet, & Pernier, 1995; Tallon-Baudry, Bertrand, Delpuech, & Pernier, 1996). We were able to show that changing the task across experiments while keeping the perceived stimuli identical changes the early evoked gamma response, whereas other early responses as the N170 were not affected by this attentional variable. Similar changes of early evoked gamma activity with task changes have been found in MEG recordings (Herrmann & Mecklinger, 2000). This indicates that early evoked gamma activity reflects a top-down mechanism involved in selecting the proper response to a stimulus that cannot be purely sensory in origin. In order to differentiate targets from non-targets, both features of a stimulus (form and collinearity) have to be compared to a template in working memory. It has been shown in simulations that high-speed access to working memory may operate at frequencies in the gamma range (Jensen & Lisman, 1998). Furthermore, Burle and Bonnet (2000) showed behavioural data from an auditory interference task, which also suggest an oscillatory process in working memory. Elliott and Müller (2000) showed that the representation of visual objects in working memory is accomplished by gamma oscillations. Therefore, the presence of a template in working memory may be critical for the generation of gamma activity in our task.

A model that accounts for our pattern of results can be sketched as follows: The plain access to working memory itself is probably not a candidate for generating the gamma response, since the amplitude of gamma activity varies for different stimuli and there is no apparent reason why the strength of memory access should vary across stimuli. But the process that compares the perceived stimuli with the template in working memory may well be the generator of the gamma activity. We demonstrated that within the three non-target stimuli the stimulus that is dissimilar to the target stimulus in two features (Kanizsa triangle) is processed faster than those that differ in only one feature. This indicates that the comparison process seems to operate as a two-fold process,

separately comparing the two features of which a target is composed. Whenever one of these two comparisons yields a positive result (Kanizsa square and non-Kanizsa triangle), this results in enhanced gamma activity as compared to both comparisons yielding negative results (Kanizsa triangle). When both comparisons yield positive results (non-Kanizsa square), we see the maximal amount of gamma activity. Thus, it seems plausible to assume that a positive comparison with working memory leads to a reinforced feedback of the frequency at which the process operates anyway, i.e., the 40 Hz are amplified more the better a perceived stimulus matches the template. This activity could then propagate to cortical areas that are relevant for correct task performance.

A further interesting result of our EEG and RT experiments was that the early evoked gamma activity correlates significantly with RTs, even though both measures were taken in different experiments. Thus, the gamma activity which peaks around 100 ms is an indicator for the much later motor reaction (approximately 600 ms). It has been reported previously that finger movements are accompanied by 40 Hz activity in the motor cortex (Pfurtscheller, Flotzinger, & Neuper, 1994). Therefore, it seems likely that early evoked gamma activity can be functionally related with motor gamma activity. Due to the additional fact that the evoked gamma activity is highly synchronized to the stimulus (evoked gamma), we think that the process underlying the correlation of early evoked gamma activity and the motor reaction is what Roelfsema, Engel, König, and Singer (1997) have described as visuomotor integration. Roelfsema et al. found highly synchronized gamma activity with zero time-lag between visual and motor areas in cats. If the selection process accessing working memory and the motor process both operate at 40 Hz, this constitutes an ideal mechanism for effective information transmission. Therefore, we render it important for future experiments to investigate the correlation of early evoked gamma activity and later motor gamma activity.

In the results of Herrmann et al. (1999) and Herrmann and Mecklinger (2000) the early evoked gamma activity was distributed more frontally than in this experiment. An unexpected result of this study was the rather occipital topography of the early evoked gamma activity. Further experiments will be needed to investigate the topography of the early evoked gamma activity in detail.

REFERENCES

- Başar-Eroglu, C., Strüber, D., Schürmann, M., Stadler, M., & Başar, E. (1996). Gamma-band responses in the brain: A short review of psychophysiological correlates and functional significance. *International Journal of Psychophysiology*, *24*, 101–112.
- Burle, B., & Bonnet, M. (2000). High-speed memory scanning: A behavioural argument for a serial oscillatory model. *Cognitive Brain Research*, *9*, 327–337.
- Donchin, E., & Coles, M.G.H. (1988). Is the P300 component a manifestation of context updating? *Behavioural Brain Science*, *11*, 357–374.

- Elliott, M.A., Herrmann, C.S., Mecklinger, A., & Müller, H.J. (2000). The loci of oscillatory visual-object priming: A combined electroencephalographic and reaction-time study. *International Journal of Psychophysiology*, 38(3), 225–242.
- Elliott, M.A., & Müller, H.J. (1998). Synchronous information presented in 40-Hz flicker enhances visual feature binding. *Psychological Science*, 9(4), 277–283.
- Elliott, M.A., & Müller, H.J. (2000). Evidence for a 40 Hz oscillatory short-term visual memory revealed by human reaction-time measurements. *Journal of Experimental Psychology Learning, Memory and Cognition*, 26(3), 703–718.
- Gray, C.M., König, P., Engel, A.K., & Singer, W. (1989). Oscillatory response in the cat visual cortex exhibit intercolumnar synchronization which reflects global stimulus properties. *Nature*, 338, 334–337.
- Heinze, H.J., Mangun, G.R., Burchert, W., Hinrichs, H., Scholz, M., Münte, T.F., Gös, A., Scherg, M., Johannes, S., Hundeshagen, H., Gazzaniga, M.S., & Hillyard, S.A. (1994). Combined spatial and temporal imaging of brain activity during visual selective attention in humans. *Nature*, 372, 543–546.
- Herrmann, C.S. & Mecklinger, A. (2000). Magnetoencephalographic responses to illusory figures: Early evoked gamma is affected by processing of stimulus features. *International Journal of Psychophysiology*, 38(3), 265–281.
- Herrmann, C.S., Mecklinger, A., & Pfeiffer, E. (1999). Gamma responses and ERPs in a visual classification task. *Clinical Neurophysiology*, 110(4), 636–642.
- Jensen, O., & Lisman, J. (1998). An oscillatory short-term memory buffer model can account for data on the Sternberg task. *Journal of Neuroscience*, 18(24), 10688–10699.
- Kanizsa, G. (1976). Subjective contours. *Scientific American*, 234(4), 48–52.
- Karakaş, S., & Başar, E. (1998). Early gamma response is sensory in origin: A conclusion based on cross-comparison of results from multiple experimental paradigms. *International Journal of Psychophysiology*, 31, 13–31.
- Mecklinger, A., & Ullsperger, P. (1993). P3 varies with stimulus categorization rather than probability. *Electroencephalography and Clinical Neurophysiology*, 86, 395–407.
- Müller, M.M., Gruber, T., & Keil, A. (2000). Modulation of induced gamma band activity in the human EEG by attention and visual processing. *International Journal of Psychophysiology*, 38(3), 283–300.
- Oken, B.S., & Chiappa, K.H. (1986). Statistical issues concerning computerized analysis of brain-wave topography. *Annals of Neurology*, 19, 493–494.
- Pachella, R.G. (1974). The interpretation of reaction time in information processing research. In B. Kantowitz (Ed.), *Human information processing*. Hillsdale, NJ: Lawrence Erlbaum Associates Inc.
- Pfurtscheller, G., Flotzinger, D., & Neuper, C. (1994). Differentiation between finger, toe and tongue movement in man based on 40 Hz EEG. *Electroencephalography and Clinical Neurophysiology*, 90, 456–460.
- Pomerantz, J.R. (1983). Global and local precedence: Selective attention in form and motion preception. *Journal of Experimental Psychology: General*, 112, 516–540.
- Pulvermüller, F., Keil, A., & Elbert, T. (1999). High-frequency brain activity: Perception or active memory. *Trends in Cognitive Science*, 3(7), 250–252.
- Roelfsema, P.R., Engel, A.K., König, P., & Singer, W. (1997). Visuomotor integration is associated with zero time-lag synchronization among cortical areas. *Nature*, 385, 157–161.
- Singer, W., & Gray, C.M. (1995). Visual feature integration and the temporal correlation hypothesis. *Annual Reviews in Neuroscience*, 18, 555–586.
- Tallon, C., Bertrand, O., Bouchet, P., & Pernier, J. (1995). Gamma-range activity evoked by coherent visual stimuli in humans. *European Journal of Neuroscience*, 7, 1285–1291.
- Tallon-Baudry, C., & Bertrand, O. (1999). Oscillatory gamma activity in humans and its role in object representation. *Trends in Cognitive Science*, 3(4), 151–162.

- Tallon-Baudry, C., Bertrand, O., Delpuech, C., & Pernier, J. (1996). Stimulus specificity of phase-locked and non-phase-locked 40 Hz visual responses in human. *Journal of Neuroscience*, *16*(13), 4240–4249.
- Teichner, W.H., & Krebs, M.J. (1974). Laws of visual choice reaction time. *Psychological Reviews*, *81*(1), 75–98.
- Tiitinen, H., Sinkkonen, J., Reinikainen, K., Alho, K., Lavikainen, J., & Näätänen, R. (1993). Selective attention enhances the auditory 40-Hz transient response in humans. *Nature*, *364*, 59–60.
- von der Malsburg, C., & Schneider, W. (1986). A neural cocktail-party processor. *Biological Cybernetics*, *54*, 29–40.
- Zeki, S. (1993). *A vision of the brain*. Oxford, UK: Blackwell Scientific Publications.